

DEVELOPMENT OF A SOLID-STATE POSITION SENSITIVE NEUTRON DETECTOR PROTOTYPE BASED ON ^6Li - GLASS SCINTILLATOR AND DIGITAL SiPM ARRAYS

S. Kumar ^a, M. Herzkamp ^a, D. Durini ^{a, b}, H. Nöldgen ^a, S. van Waasen ^{a, c}

^a *Central Institute of Engineering, Electronics and Analytics ZEA-2 – Electronic Systems,
Forschungszentrum Jülich GmbH, 52425 Jülich, Germany*

^b *Department of Electronics, National Institute of Astrophysics, Optics and Electronics (INAOE),
Tonatzintla, 72840 Puebla, Mexico*

^c *Faculty of Engineering, Communication Systems (NTS), University of Duisburg-Essen, 47057
Duisburg, Germany*

Abstract— Photomultiplier tubes (PMT) have been used extensively as the photodetector of choice in scintillation based detectors for cold and thermal neutrons. However, the limitations of PMT based scintillation neutron detectors such as their sensitivity to magnetic fields or their high operating voltages (> 1 kV) have triggered the search for alternative photodetectors for these applications. Silicon photomultipliers (SiPM) operate in the single photon regime, have lower operating voltages (~ 20 - 70 V) than PMTs and are insusceptible to magnetic field. Additional features of the SiPMs like their low production cost, compactness and higher readout rates make them a potential candidate to replace the photodetector part in these developments. Therefore, we are developing a scintillation neutron detector based on SiPM technology. The detector prototype with an active detection area of 13 cm × 13 cm is aimed to be used in the future at the *TREFF* instrument of the *Heinz Maier-Leibnitz Zentrum (MLZ)* in Garching, Germany, for neutron reflectometry experiments. In this paper, we report the detector concept, its development and the simulation results for design optimization.

Keywords: Neutron scintillation detectors, Silicon Photomultipliers (SiPM), Cold and thermal neutrons, Geant4

26

1. INTRODUCTION

27 Neutron-sensitive ^6Li scintillator glass has been used since the 1950s to detect thermal and cold
28 neutrons [1]. The light produced due to capturing of neutrons in the scintillator is detected by
29 photodetectors. Conventionally, vacuum photomultiplier tubes (PMTs) are used for this [2]. However, the
30 limitations of PMTs such as their inability to operate in magnetic fields, their intrinsic high voltage
31 requirement (hundreds of volts), and the electromechanical complexity of their installation compelled us to
32 test a new technology for this kind of applications: the silicon photomultipliers (SiPM), also known as
33 Geiger-mode avalanche photodiodes [3] [4]. A SiPM usually consists of a matrix of thousands of
34 independent single photon avalanche photodiode (SPAD) cells per mm^2 connected in parallel. Each cell is
35 coupled with a quenching mechanism, either passively (in case of analog SiPMs) or actively (for digital
36 SiPMs) and is designed to operate above the breakdown voltage to detect extremely low light intensity
37 down to a single photon. Some advantages of these solid-state photodetectors over PMTs are their relatively
38 low operation cost, much lower operating voltages, compactness, and their operability in magnetic fields up
39 to several Tesla. The main concern of using this technology in neutron detection is radiation damage, which
40 we studied in detail recently [5] [6]. In the said study, we concluded that SiPMs can be used for cold /
41 thermal neutron detection in typical Small Angle Neutron Scattering (SANS) experiments without
42 significant performance degradation during 10 or more years of constant operation. Motivated by these
43 findings, we are currently developing a $13\text{ cm} \times 13\text{ cm}$ novel scintillation neutron detector prototype based
44 on *Philips Digital Photon counter* (PDPC) digital SiPM arrays. The targeted spatial resolution of the
45 scintillation prototype and its neutron counting rate are $1\text{ mm} \times 1\text{ mm}$ and 20 Mcps/ m^2 respectively. In this
46 work we focused on finding the optimum design, to achieve the aimed resolution. For this, we performed
47 some simulations and based on the results obtained we choose the desired configuration.

48

2. DETECTOR DESIGN

49 The detector consists of three subsystems: the optical front-end, the readout electronics, and the cooling
50 system. The schematic of the entire detector comprising its sub-systems is depicted in Fig. 1. The optical

front-end consists of a scintillator glass which converts cold neutrons into light (300 - 500 nm), a disperser glass (*PGO- D263 T eco* [7]) which spreads the light across several pixels of PDPC for a better position reconstruction of impinging neutrons, and a PDPC array used to detect this visible light produced within the scintillator glass. We use 1 mm thick GS20®, a Cerium activated (Ce^{3+}) monolithic scintillator glass enriched with ^6Li to 95%, from *Scintacor* [8]. The adhesive used, between disperser glass and SiPM was *Panacol-Vitralit 1605* [9] glue and, between scintillator glass and disperser glass was *Eljen EJ-552* [10] gel. One of the four underlying PDPC modules (see Fig. 2) comprises an array of 2×2 *DPC3200-22-44* [11] tiles and each tile is divided into 8×8 SiPMs (referred to as pixels here) with a 4 mm pitch. Each pixel (with a photoactive area of $3.8 \text{ mm} \times 3.2 \text{ mm}$) contains 3200 photosensitive avalanche diodes (referred to as photoactive cells) operating in the Geiger-mode. Every 2×2 array of pixels forms a die, which is an independent readout unit. The optical front-end is additionally covered by an aluminum cap to prevent any stray light from entering the detector. The readout mechanism is similar to the one thoroughly described in [12] and gives an output, within a die, in terms of number of photons detected in each pixel. In order to keep the thermal noise (amount of dark counts) of the PDPC modules at a steady level, a cooling system maintains them at a constant temperature of 14°C . The cooling system (see Fig. 1) consists of two Peltier elements (*Eureca - TECISE-55-55-280/78*) and a heat sink attached to a fan.

3. DETECTOR PRINCIPLE

The mechanism behind the detection of neutron by a GS20® glass is based upon scintillation i.e. it converts energy of a neutron into a number of photons in the near visible range. Whenever a thermal or cold neutron reacts with lithium-6 isotope, it produces charged particles alpha particle and tritium (^3H) with associated kinetic energies (see reaction 1). Any of the resultant (tritium and α) interaction with the Ce^{3+} activator, that offers high light yield and fast response due to its dipole $5d - 4f$ transition, leads to ionization in Cerium atoms through partially transferred energy. This excited cerium, in the process of de-excitation, emits isotropic light (transparent to the scintillator), e.g. ~ 6000 photons with a decay time between 50 to 70 ns for a neutron having wavelength of 1.8 \AA [8], which is be detected by the underlying photodetector (see Fig. 3).

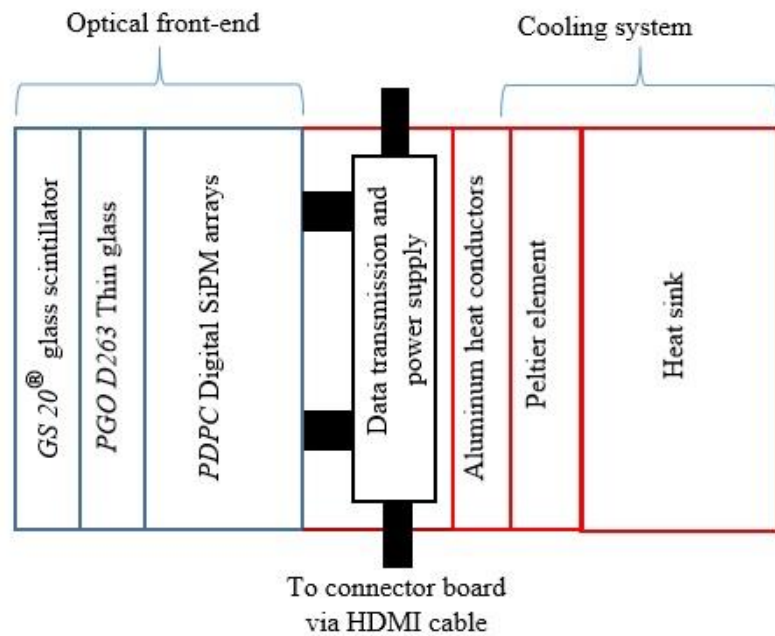


Figure 1: Sketch of the detector design. (color online)

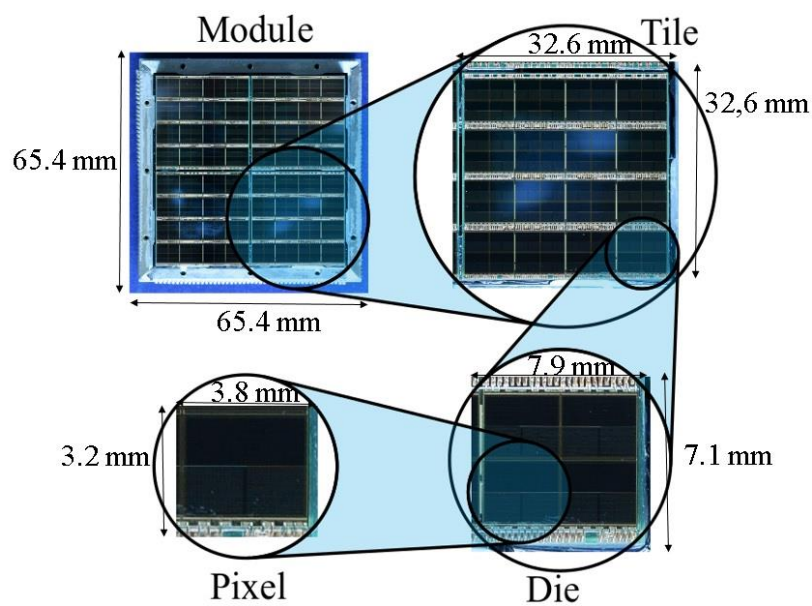


Figure 2: Diagram of a PDPC module along with its subdivision into tile (2x2), further into (4x4) die and subsequently into (2x2) pixel. (color online)

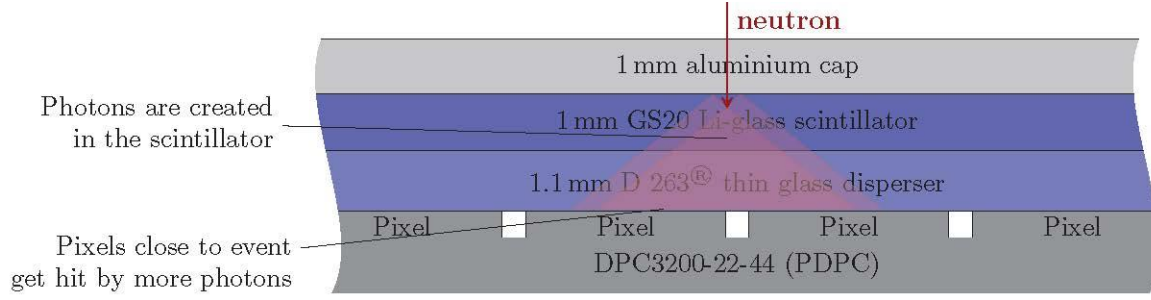
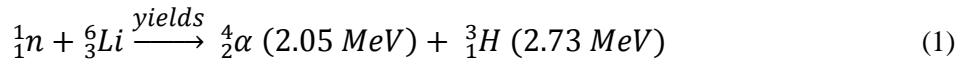


Figure 3: Representation of a neutron capture in the scintillator and propagation of light to the PDPC through the glass. To increase signal to noise ratio the aluminum cap is polished that reflects some of the photons directed away back to the PDPC. (color online)



The absorption length of α particle is 5-10 μm and for tritium is 40-150 μm that means that the position of the impinged neutron can be traced with an uncertainty of $\pm 150 \mu\text{m}$ [13]. The peak wavelength of the scintillator emission is 390 nm, which corresponds to the photon detection efficiency (PDE) of approximately 30 % achieved by the PDPC at the same wavelength. As it can be observed in Fig. 4, the peak detection efficiency of 45 % is reached by the PDPC at 420 nm wavelength, which is an acceptable match.

The mathematical reconstruction of the exact position where the detected cold neutron impinged the scintillation glass used is based on the analysis of the proportional amount of detected photons in different PDPC pixels following the original proposal made by Anger in 1958 [14]. The approach is to fit the detector response function to the measured data. We estimated a pixel's response to a neutron event at the lateral position (x, y) by integrating the photon distribution function obtained in simulations over the geometric area of the pixel centered on (x, y). Early tests with a demonstrator device suggest that a two dimensional resolution of 1 mm is possible using this approach and further optimization of neutron positioning algorithm is in progress and will be reported in near future.

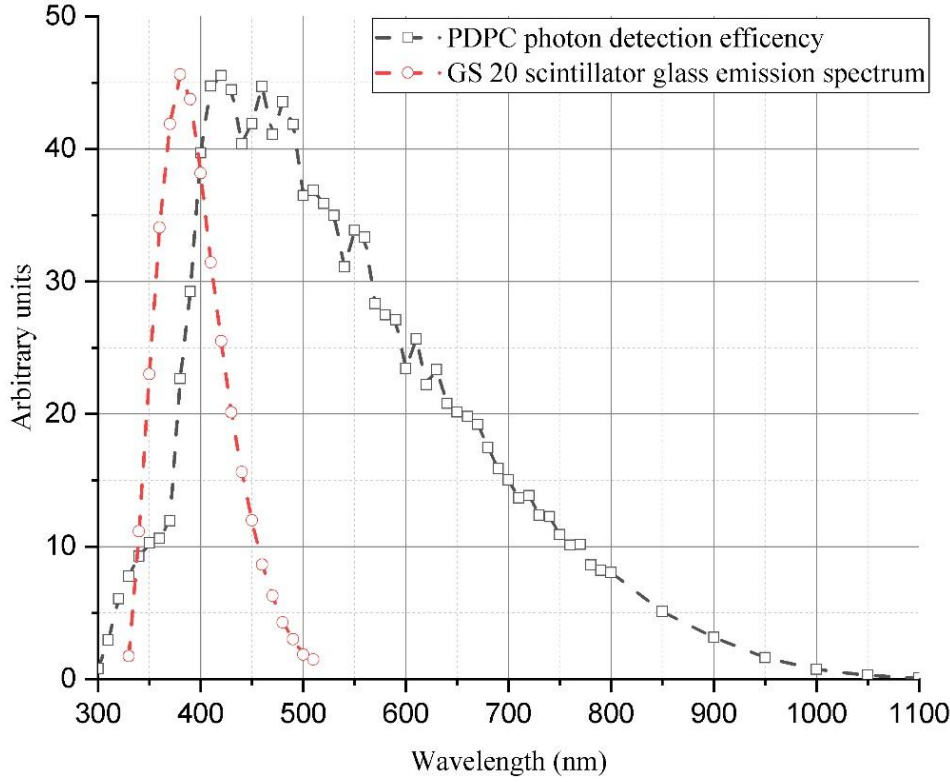


Figure 4: Graph showing the comparison of GS20® scintillator glass emission spectrum for thermal neutrons and photon detection efficiency of the PDPC sensor. The sensor has ~30 % PDE at 395nm, the peak light emission of the scintillator, and ~31 % PDE averaged across the whole emission spectrum. (color online)

4. OPTICAL FRONT END SIMULATION

In order to increase the position accuracy we emphasized on the optimization of the optical-front end design, considering the thickness of scintillator glass and disperser glass. For this purpose we conducted Geant4 0 simulations of the optical setup, to examine their influences towards reaching the desired specification. For each parameter set (scintillator yield of 6000 photons / neutron, yield ratio of 0.5, fast and slow decay time = 50 ns and 70 ns, scintillator refractive index = 1.55, beam width = 1mm etc.) we simulated 10,000 neutron ($\lambda = 4.78 \text{ \AA}$, $E = 3.58 \text{ meV}$) beam impinging the detector surface perpendicularly. Neutron interaction with matter was simulated by including the G4HadronPhysicsFTFP_BERT_HP physics list. Furthermore, we

included G4EmStandardPhysics for energy deposition by the alpha and tritium particles, and G4OpticalPhysics for the propagation of photons. We also simulated the gel and the glue, considering their thickness (100 μm) and refractive indices of 1.47 and 1.52 respectively, which were chosen to match with the scintillator's refractive index (1.55) for an efficient scintillation light transport at the interfaces. The interfaces were described as dielectric-metal and dielectric-metalloid boundaries, other than the default interfaces. The scintillator thickness (1mm) was chosen such that, to have a balance between high neutron converting efficiency and low sensitivity towards gamma rays [16]. The relative composition of the scintillator considered for the simulation is given in the table 1.

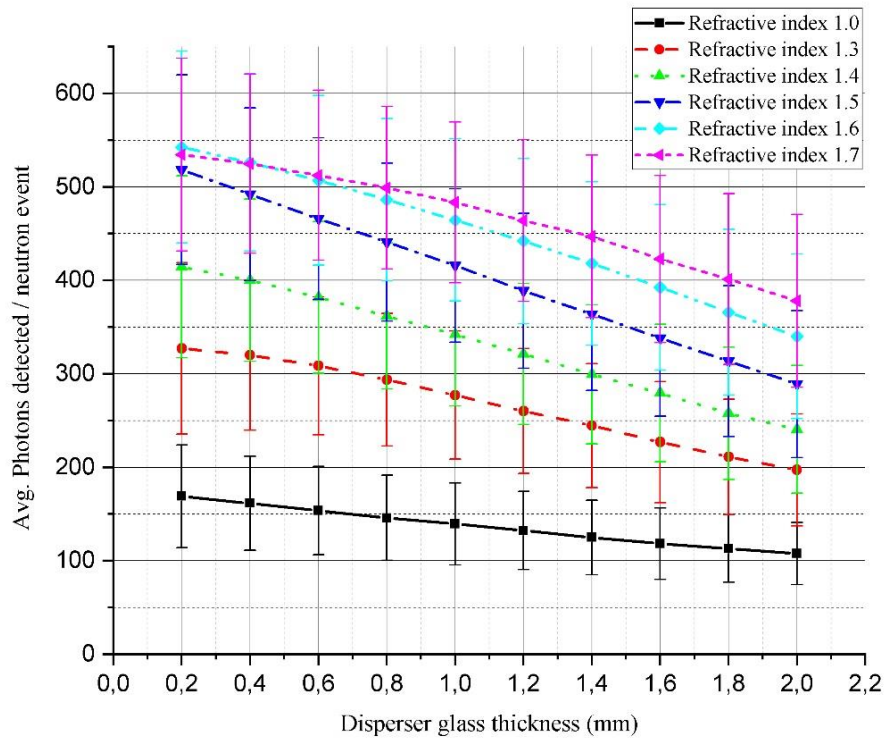
Compounds	Li_2O	Al_2O_3	MgO	Si_2O_3	Ce_2O_3
Mass Composition	0.157	0.603	0.169	0.034	0.037

Table 1: Composition of the GS20® ^6Li scintillator glass, considered for the Geant4 simulation.

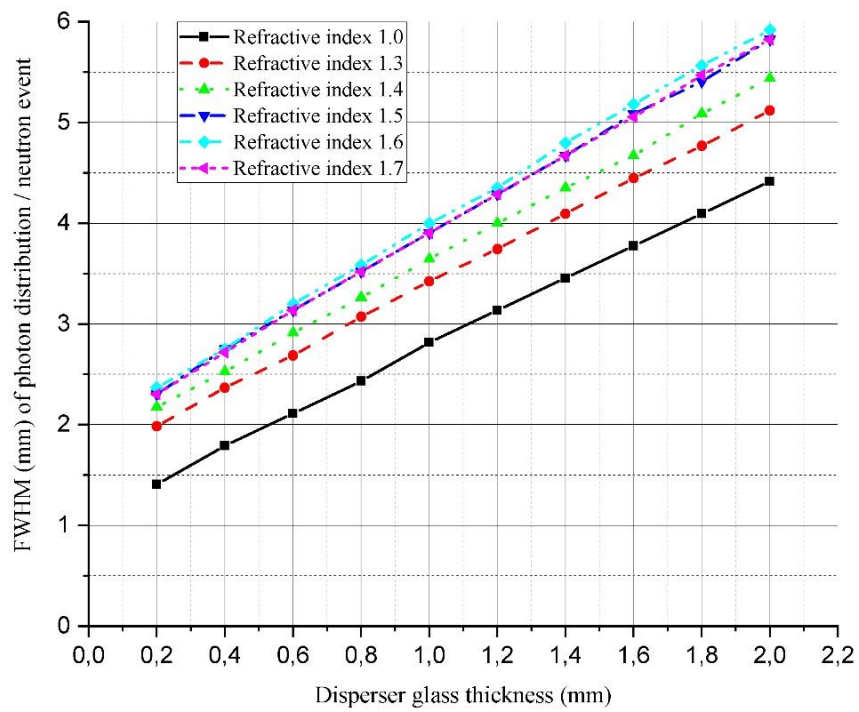
In case of a neutron capture, photons are created with random direction and wavelength according to the emission spectrum of lithium-glass. For each event the position and time of any photon, hitting the SiPM surface is stored for analysis. The geometry and performance of the PDPC pixels, as well as the readout cycle chosen, are taken into account during the data analysis.

A certain distribution of light across several pixels is necessary for a position reconstruction with sub-pixel accuracy, which favors a thicker disperser glass. However, increasing the thickness also reduces the amount of photons detected per pixel, and thus, events might be discarded for not fulfilling the threshold condition which discriminates against gamma events and noise.

Fig. 5 (a) shows the dependence of the average number of triggered cells during a simulated neutron event on the disperser thickness and its refractive index. Higher thickness leads to a smaller number of triggered cells, because the photon density on the PDPC surface decreases. A lower refractive index has a similar effect, because it increases the refraction angle. However, refractive indices below 1.55 (refractive index of the GS20® lithium glass used) not only reduce the photon density, but also the amount of photons entering



(a)



(b)

Figure 5: Geant4 simulation results, using 1 mm thick scintillator glass, for the influence of disperser glass thickness and the refractive index on (a) the average number of photons detected, and (b) the full width at half-maximum (FWHM) value of the photon distribution on PDPC surface. (color online)

the disperser glass due to the total internal reflection at the surface between the lithium glass and the disperser glass.

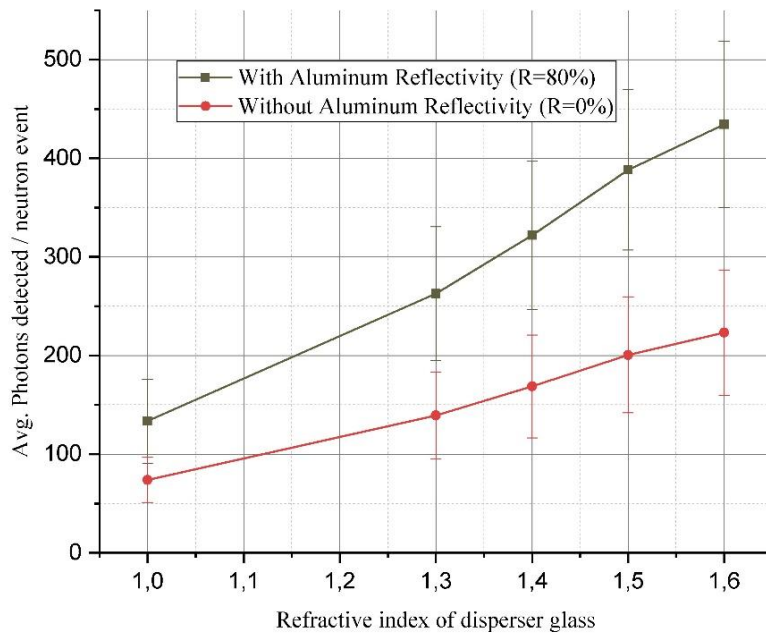
The full width at half maximum (FWHM) of the photon distribution is shown in Fig. 5 (b). For this analysis, all photons incident on the PDPC were considered, disregarding the PDPC geometrical properties and its PDE. Here, the refractive index has a saturating influence, as the curves for 1.5, 1.6 and 1.7 almost coincide with each other. The influence of the disperser thickness on the FWHM is linear, as can be expected for geometric reasons. For a sufficient photon distribution, the FWHM should be of the order of the pixel pitch (4 mm), while the number of detected photons should be as high as possible. Therefore, we decided to use a 1 mm thick disperser glass with a refractive index of 1.5.

Further simulations were performed to assess the effect of polishing the aluminum cap versus making it light absorbing. Fig. 6 (a) and (b) shows that polishing the cap almost doubles the number of detected photons and increases the FWHM by ~ 0.5 mm, respectively.

5. CONCLUSION AND OUTLOOK

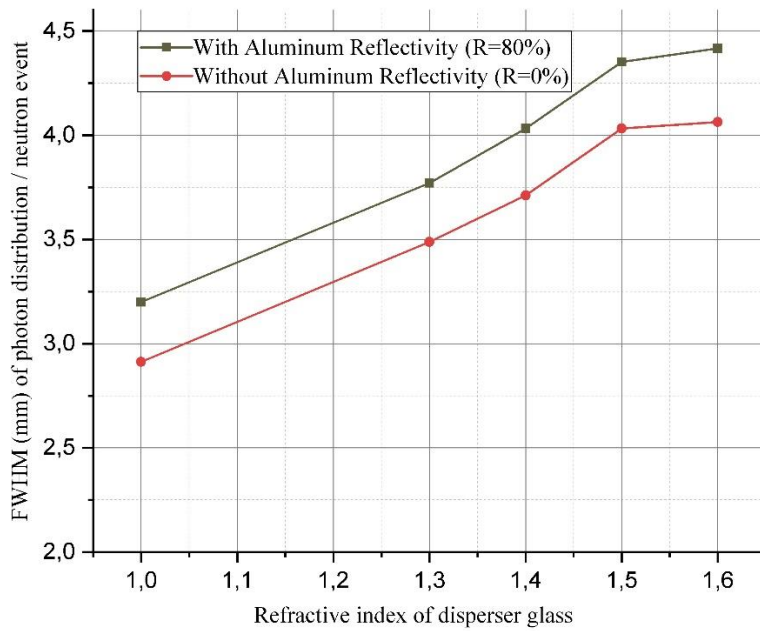
In this paper, we have introduced a novel concept for a position-sensitive neutron scintillator detector using SiPM arrays. Using GS20®, a ^6Li glass activated with cerium(Ce^{3+}), together with a SiPM as underlying photodetector allow the development of an advanced, compact and scalable potential detector alternative, operating at only few tens of volt and also in high magnetic field. However, its development requires a suitable design to achieve a two dimensional resolution of $1 \text{ mm} \times 1 \text{ mm}$. This was accomplished by optimizing the optical front-end design by means of Geant4 simulation. We simulated the entire optical set up: a GS20® scintillator glass interfacing a disperser glass, through a gel, that is glued on SiPM arrays and an aluminium cap covering them. The simulations were aimed at achieving enough light distribution on the

163



164

(a)



165

(b)

166

Figure 6: Difference of (a) number of photons detected by the PDPC and (b) full width at half-maximum value (FWHM) of photon distribution, for reflective and absorbing aluminum cap. Thickness of disperser glass was 1 mm of refractive index 1.5 and scintillator glass was 1 mm. (color online)

167

168

SiPM surface so that the light of any neutron event is distributed among more than one pixel. This way, the position of a neutron event can be reconstructed to a higher precision than the pixel pitch (4 mm).

Using the average number of photons detected by the SiPM array per neutron event and the FWHM of their distribution on the SiPM surface with respect to a neutron position as figures of merit, our simulations suggest that a 1-mm-thick monolithic GS20® scintillator glass along with a 1-mm-thick disperser glass having a matching refractive index and a polished aluminium cap is a good candidate configuration to aim for a resolution of 1 mm × 1 mm.

The detector prototype presented in this work will be tested at the TREFF instrument at the Heinz Maier-Leibnitz Zentrum (MLZ), Garching, Germany, using a dedicated reconstruction algorithm to precisely locate the position of a neutron within 1 mm. The measurements will assess the achieved position resolution and counting capabilities of the detector, and support the validation of our models and simulation results.

References

- [1] V.K. Voitovetskii, N.S. Tolmacheva and M.I. Arsaev, *Atomnaya Energ.* 5 (1959) 321 and *Atomnaya Energ.* 6 (1959) 472
- [2] R. Riedel, C. Donahue, T. visscher, C. Montcalm “Design and performance of a large area neutron sensitive anger camera” *Nuclear Instruments and Methods in Physics Research A* 794 (2015) , p.224
- [3] Z. Sadygov, RU 2102820,1996
- [4] V. Golovin, RU 2142175, 1998
- [5] D. Durini et al “Evaluation of the dark signal performance of different SiPM-technologies under irradiation with cold neutrons” *Nuclear Instruments and Methods in Physics Research A* 835 (2016) , p. 99
- [6] S. Kumar, D. Durini, C. Degenhardt, S. van Waasen “Photodetection characterization of SiPM technologies for their application in scintillator based neutron detectors” *Journal of Instrumentation* Vol. 13 (2018) C01042
- [7] Thin glass available at <https://www.pgo-online.com/intl/D263.html> (accessed on July, 2018)
- [8] 6-lithium scintillator glass available at <https://scintacor.com/products/6-lithium-glass/> (accessed on July, 2018)
- [9] UV and light curing adhesives available at <https://www.panacol.com/products/adhesive/vitralit/> (accessed on July, 2018)
- [10] Silicon grease available at <https://eljentechnology.com/products/accessories/ej-550-ej-552> (accessed on July, 2018)
- [11] T. Frach, G. Prescher, C. Degenhardt, R. Gruyter, A. Schmitz, R. Ballizany “The digital silicon photomultiplier – principle of operation and intrinsic detector performance” *Proc. IEEE Nuclear Science Symposium Conference*, Orlando, Florida 2009, pp. 1959–1965.
- [12] H. Nöldgen et al “Read-out electronics for Digital Silicon Photomultiplier Modules”, *Proc. IEEE Nuclear Science Symposium Conference*, Seoul, South Korea 2013, M16-46
- [13] C.W.E. van Eijk, A. Bessière, P. Dorenbos, “Inorganic thermal-neutron scintillators”, *Nuclear Instruments and Methods in Physics Research Section A* 529 (2004), pp. 260–267
- [14] H. O Anger, “Scintillation camera” *Review of Scientific Instruments*, Vol. 29, No. 1, 1958, p.27
- [15] S. agostinelli et al “GEANT4- a simulation toolkit” *Nuclear Instruments and Methods in Physics Research A* 506 (2003) , p.50

211 [16] D Harris, C Duffill and L.A Wraight, "Inelastic Scattering of Neutrons in Solids and Liquids" 1 (IAEA
212 1963) 171